

The chemical composition of the Sun from helioseismic and solar neutrino data

Francesco L. Villante^{1,2}, Aldo M. Serenelli³, Franck Delahaye⁴ and Marc H. Pinsonneault⁵

¹*Dipartimento di Scienze Fisiche e Chimiche, Università dell'Aquila, 67100 L'Aquila, Italy*

²*Istituto Nazionale di Fisica Nucleare (INFN), Laboratori Nazionali del Gran Sasso (LNGS),
67100 Assergi (AQ) , Italy*

³*Instituto de Ciencias del Espacio (CSIC-IEEC), Facultad de Ciencias, 08193 Bellaterra, Spain*

⁴*LERMA, Observatoire de Paris, ENS, UPMC, UCP, CNRS, 92190 Meudon, France*

⁵*Astronomy Department, Ohio State University, Columbus, Ohio 43210, USA*

ABSTRACT

We perform a quantitative analysis of the solar composition problem by using a statistical approach that allows us to combine the information provided by helioseismic and solar neutrino data in an effective way. We include in our analysis the helioseismic determinations of the surface helium abundance and of the depth of the convective envelope, the measurements of the ^7Be and ^8B neutrino fluxes, the sound speed profile inferred from helioseismic frequencies. We provide all the ingredients to describe how these quantities depend on the solar surface composition and to evaluate the (correlated) uncertainties in solar model predictions. We include errors sources that are not traditionally considered such as those from inversion of helioseismic data. We, then, apply the proposed approach to infer the chemical composition of the Sun. We show that the opacity profile of the Sun is well constrained by the solar observational properties. In the context of a two parameter analysis in which elements are grouped as volatiles (i.e. C, N, O and Ne) and refractories (i.e Mg, Si, S, Fe), the optimal composition is found by increasing the the abundance of volatiles by $(45 \pm 4)\%$ and that of refractories by $(19 \pm 3)\%$ with respect to the values provided by Asplund et al. (2009). This corresponds to the abundances $\varepsilon_{\text{O}} = 8.85 \pm 0.01$ and $\varepsilon_{\text{Fe}} = 7.52 \pm 0.01$. As an additional result of our analysis, we show that the observational data prefer values for the input parameters of the standard solar models (radiative opacities, gravitational settling rate, the astrophysical factors S_{34} and S_{17}) that differ at the $\sim 1\sigma$ level from those presently adopted.

Subject headings: Sun: helioseismology - Sun: interior - Sun: abundances - neutrinos

1. Introduction

In the last three decades, there has been enormous progress in our understanding of stellar structure and evolution. Solar models have played a particularly important role, in large part because we have powerful diagnostics of the internal solar conditions from solar neutrino experiments and helioseismology. The deficit of the observed solar neutrino fluxes relative to solar model predictions, initially reported by Homestake (Davis et al. 1968) and then confirmed by GALLEX/GNO (Hampel et al. 1999; Altmann et al. 2005), SAGE (Abdurashitov et al. 1999), Kamiokande (Hirata et al. 1989) and Super-Kamiokande (Cravens et al. 2008), SNO (Ahmad et al. 2002) and Borexino (Arpesella et al. 2008), gave rise to the solar neutrino problem: major changes were required in either the theory of stellar structure and evolution and neutrino physics. The development, refinement, and testing of the Standard Solar Model (SSM) played an important role in its ultimate resolution in 2002¹, when the SNO experiment obtained direct evidence for flavor oscillations of solar neutrinos and confirmed the SSM prediction of the ^8B neutrino flux with a precision that, according to the latest data, is equal to about 3%.

The Sun is a non-radial oscillator, and powerful insights have also emerged from the study of the solar frequency pattern (for example, see Basu & Antia (2008)). The sound speed as a function of depth can be reconstructed to high precision, of order 0.1%. Abrupt changes in the solar thermal structure from ionization and the transition from radiative to convective energy transport induce acoustic glitches that can be precisely localized; we can therefore infer the depth of the convective envelope at the 0.2% level and the surface helium abundance at the 1.5% level. As a result, the solar structure is now well constrained and the Sun can be used as a solid benchmark for stellar evolution and as a *laboratory* for fundamental physics (see e.g. Fiorentini et al. (2001); Ricci & Villante (2002); Bottino et al. (2002)). In fact, it was the excellent agreement between solar models and helioseismic inferences on the solar structure (better than 1.5σ for all constraints) that gave a strong support to the idea that the root of the *solar neutrino problem* had to be found outside the realm of solar modelling (Bahcall et al. 2001), before evidence for neutrino oscillations was found.

All these important measurements acquire even more relevance when considering that, in recent years, a *solar composition problem* has emerged. The SSM treats the absolute and relative elemental abundances as an input, and the Grevesse & Sauval (1998) (hereafter GS98) mixture yields concordance between model and data. Relative abundances of heavy elements can be precisely measured in meteorites (Lodders 2010), but the abundances of the important light CNO elements can only be measured in the photosphere. The Ne abundance is even less secure, as it is inferred from solar wind measurements. A systematic overhaul in solar model atmospheres, see Asplund et al. (2005) and Asplund et al. (2009) (hereafter AGSS09), has led to a downward revision in the inferred

¹For the sake of precision, the first model-independent evidence for solar neutrino oscillations and the first determination of the ^8B solar neutrino flux has been obtained in 2001 (see Fogli et al. (2001)) by comparing the SNO charged-current result (Ahmad et al. 2001) with the SK data with the method proposed by Villante et al. (1999). The year 2002 is, however, recognized as the ‘annus mirabilis’ (Fogli et al. 2003) for the solar neutrino physics.

photospheric heavy element abundances (see Table 1) by up to 30-40% for important species such as oxygen. The magnitude of the differences is model(er) dependent; independent measurements by Caffau et al. (2011) (see also Lodders (2010)) are intermediate between the GS98 and AGSS09 scales. The internal structure of SSMs using the lower solar surface metallicity of AGSS09 does not reproduce the helioseismic constraints; for example, the sound speed disagrees at the bottom of the convective envelope by about $\sim 1\%$ with the value inferred from helioseismology. In addition, the predicted surface helium abundance is lower by $\sim 7\%$ and the radius of the convective envelope is larger by $\sim 1.5\%$ with respect to the helioseismic results. In synthesis, inferences from modern three-dimensional hydrodynamic models of the solar atmosphere lead to predictions for the solar interior that are in strong disagreement with observational constraints, well above the currently estimated errors.

The solar composition problem has been addressed by a number of independent interior calculations. Problems in reconciling helioseismic data with a low abundance scale became obvious early on (Basu & Antia (2004); Bahcall & Pinsonneault (2004); Turck-Chièze et al. (2004)). Bahcall et al. (2006) performed a Monte Carlo analysis that included calculations of the RMS deviations between the inferred solar sound speed profile and that predicted by models with the "high" and "low" abundances. Delahaye & Pinsonneault (2006) advocated an inversion of the problem, solving for the abundances consistent with the base of the surface convection zone and surface helium abundance. The ionization signature in the surface convection zone can also be used as an independent diagnostic suggesting high metallicity (see, however, discussion in Vorontsov et al. (2013)); Basu & Antia (2008) summarized the initial results favoring a higher solar metallicity. Physical processes not included in the standard model could potentially provide an explanation, but the combination of constraints has proven difficult to reproduce in practice (Guzik & Mussack 2010). An intermediate solar metallicity using low-degree modes was reported by Houdek & Gough (2011); however, these authors note that their mixture produces a sound speed profile at variance with solar data.

The goal of this work is to perform a complete and quantitative analysis of the solar composition problem. In particular, we address the following questions: which is the chemical composition of the Sun that, by using the current input physics of solar models, can be inferred from helioseismic and solar neutrino data? How does different observational information combine in determining the optimal composition of the Sun? How does the obtained composition compare to the photospheric inferred values? Do the different observational data show tensions and/or inconsistencies that may point at some inadequacies in the SSM input parameters or assumptions? Even if the problem has been already considered in literature, a thorough self-consistent discussion is still missing. While a rigorous approach is not necessary for a qualitative assessment of the problem, it becomes essential for our goal, i.e. to use the helioseismic information in combination with the solar neutrino results to infer the properties of the Sun. In order to make a correct inference, one has to define an appropriate figure-of-merit (e.g. a χ^2 statistics) that has to be non-biased and should combine the different pieces of the observational information with the correct relative weights.

In this respect, important progress has to be done at a methodological level. This papers starts

addressing this problem. We propose to use a statistical approach, normally adopted in other areas of physics (e.g. in neutrino studies, see Fogli et al. (2002)) in which all the relevant pieces of information can be combined in a correct and effective way. We discuss a strategy to include the observational information for the sound speed profile, the radius of the convective envelope, the surface helium abundance, and the ^7Be and the ^8B neutrino fluxes. We provide all the ingredients to describe how these quantities depend on the assumed chemical composition and to evaluate the (correlated) uncertainties in solar model predictions.

The plan of the paper is as follows. In § 2, we review the status of SSM calculations, discuss in detail our treatment of uncertainties in theoretical predictions and also the observational constraints considered in the analysis, including sources of errors not traditionally considered such as those from inversion of helioseismic data. In § 3, we describe the adopted statistical approach. In § 4, we analyze the response of the Sun to variations of its surface composition. § 5 contains the results of our analysis, i.e. the bounds on the chemical composition of the Sun that are inferred from helioseismic and solar neutrino data. Finally, we provide a summary and conclusions in § 6.

2. Models and Data

Our theoretical working framework is the SSM and in § 2.1 we summarize the aspects most relevant to this work. More importantly, we present our treatment of errors, for which two qualitatively different sources must be identified. On one hand, errors in the input parameters I for solar model construction induce *theoretical* uncertainties in the SSM predictions Q . These errors are fully correlated, as it is discussed in § 2.2. On the other, the observational determinations Q_{obs} of helioseismic quantities and solar neutrino fluxes are affected by *observational* errors. In this work, we treat these errors as uncorrelated, as it is discussed in § 2.3.

2.1. Standard Solar Models

The development of a new generation of stellar atmospheres models resulted in a downward revision of the solar photospheric abundances. This is shown e.g. in Table 1 where we give the abundances of C, N, O, Ne, Mg, Si, S and Fe, which are the relevant elements for solar model construction for the (new) AGSS09 (Asplund et al. 2009) and (old) GS98 (Grevesse & Sauval 1998) heavy element admixtures. Last column shows the fractional differences between the individual abundances (relative to hydrogen) in the two compilations.

The heavy element admixture determines to a large extent the opacity profile of the Sun and is a crucial input for solar model construction. This is seen in the first two columns of Table 2, where we report the results of two recent SSM calculations (Serenelli et al. 2011) that implement the AGSS09 (Asplund et al. 2009) and GS98 (Grevesse & Sauval 1998) surface compositions. The models have been computed with GARSTEC (Weiss & Schlattl 2008), using the nuclear reaction

Element	AGSS09	GS98	δz_i
C	8.43 ± 0.05	8.52 ± 0.06	0.23
N	7.83 ± 0.05	7.92 ± 0.06	0.23
O	8.69 ± 0.05	8.83 ± 0.06	0.38
Ne	7.93 ± 0.10	8.08 ± 0.06	0.41
Mg	7.53 ± 0.01	7.58 ± 0.01	0.12
Si	7.51 ± 0.01	7.56 ± 0.01	0.12
S	7.15 ± 0.02	7.20 ± 0.06	0.12
Fe	7.45 ± 0.01	7.50 ± 0.01	0.12
Z/X	0.0178	0.0229	0.29

Table 1: Solar surface heavy element abundances in the AGSS09 (Asplund et al. 2009) and GS98 (Grevesse & Sauval 1998) admixtures. Abundances are given as $\varepsilon_j \equiv \log(N_j/N_H) + 12$, where N_j is the number density of element j . Last row gives the total metal-to-hydrogen mass fraction. In the last column, we show the fractional differences δz_j between the abundances in the two compilations.

rates recommended in Adelberger et al. (2011) and the input physics described in Serenelli et al. (2009). Element diffusion in the solar interior is included according to Thoul et al. (1994). The models have been computed by using the radiative opacities from the Opacity Project (OP; Badnell et al. (2005)), complemented at low temperatures with the opacities from Ferguson et al. (2005). We consider the following observable quantities: the surface helium abundance Y_b , the radius of the inner boundary of the convective envelope R_b , the neutrino fluxes Φ_ν , where the index $\nu = \text{pp, Be, B, N, O}$ refers to the neutrino producing reactions according to the usual convention. We also show in Figure 1 the fractional difference $\delta c_i \equiv (c_{\text{obs},i} - c(r_i)) / c(r_i)$ between the predicted sound speed $c(r)$ and the values $c_{\text{obs},i}$ inferred from helioseismic data; the black line refers the SSM model implementing the AGSS09 surface composition while the red line is obtained by using the GS98 admixture.

In the following, we take the SSM implementing the AGSS09 composition as a starting point for our analysis and we use the notation \overline{Q} (\overline{I}) to indicate the prediction (assumption) for the generic quantity Q (input I) in this calculation.

2.2. Theoretical uncertainties

The errors quoted in Table 2 and the light-blue band in Figure 1 correspond to 1σ uncertainties in theoretical predictions. They have been calculated by propagating the errors in the following input parameters: the age of the Sun (**age**); the diffusion coefficients (**diffu**); the luminosity (**lum**); the opacity profile (**opa**) of the Sun; the astrophysical factors S_{11} , S_{33} , S_{34} , S_{17} , S_{e7} and $S_{1,14}$. Note that, as we are interested in establishing bounds on the solar chemical composition,

	AGSS09	GS98	Obs.	GS98rec
Y_b	$0.2319 (1 \pm 0.013)$	$0.2429 (1 \pm 0.013)$	0.2485 ± 0.0035	0.243
R_b/R_\odot	$0.7231 (1 \pm 0.0033)$	$0.7124 (1 \pm 0.0033)$	0.713 ± 0.001	0.710
Φ_{pp}	$6.03 (1 \pm 0.005)$	$5.98 (1 \pm 0.005)$	$6.05(1^{+0.003}_{-0.011})$	5.98
Φ_{Be}	$4.56 (1 \pm 0.06)$	$5.00 (1 \pm 0.06)$	$4.82(1^{+0.05}_{-0.04})$	4.98
Φ_B	$4.59 (1 \pm 0.11)$	$5.58 (1 \pm 0.11)$	$5.00(1 \pm 0.03)$	5.49
Φ_N	$2.17 (1 \pm 0.08)$	$2.96 (1 \pm 0.08)$	≤ 6.7	2.89
Φ_O	$1.56 (1 \pm 0.10)$	$2.23 (1 \pm 0.10)$	≤ 3.2	2.15

Table 2: The predictions of SSMs implementing GS98 (Grevesse & Sauval 1998) and AGSS09 (Asplund et al. 2009) admixtures. The theoretical uncertainties have been calculated as it is described in the text and do not include the contributions due to errors in the surface composition. In the third column, we show the observational values for helioseismic quantities (Basu & Antia 2004, 1997) and solar neutrino fluxes (Bellini et al. 2011). In the last column, we calculate the GS98 solar model predictions starting from AGSS09 solar model by using the linear expansion given in equation (22). The neutrino fluxes are given in following units: $10^{10} \text{ cm}^{-2}\text{s}^{-1}$ (pp); $10^9 \text{ cm}^{-2}\text{s}^{-1}$ (Be); $10^6 \text{ cm}^{-2}\text{s}^{-1}$ (B); $10^8 \text{ cm}^{-2}\text{s}^{-1}$ (N); $10^8 \text{ cm}^{-2}\text{s}^{-1}$ (O).

we have explicitly omitted its contribution to theoretical uncertainties. By following the standard procedure, we have calculated the logarithmic derivatives

$$B_{Q,I} = \frac{d \ln Q}{d \ln I}. \quad (1)$$

$B_{Q,I}$ values are available at Serenelli et al. (2013) for all observables except the sound speed $c(r)$. To our knowledge, the logarithmic derivatives $B_{c,I}(r)$ of the sound speed, defined as

$$B_{c,I}(r) \equiv d \ln c(r) / d \ln I \quad (2)$$

have not been given elsewhere in the scientific literature and are shown in the left panel of Figure 2 as a function of the solar radius.

As mentioned before, the uncertainty δI in each input parameter I produces fully correlated errors on the SSM predictions of observables Q . To emphasize this point, we use the symbol $C_{Q,I}$ to indicate the fractional variation of Q when a fractional correction δI is applied to the input I . The various contributions $C_{Q,I}$, shown in Table 3 and in the right panel of Figure 2, are calculated from the relation

$$C_{Q,I} = B_{Q,I} \delta I \quad (3)$$

with the δI values summarized in Serenelli et al. (2013). The only exception is the opacity, that we discuss below.

Opacity is not a single number but a complicated function of the properties of the solar plasma which can be modified in a non trivial way. To take this into account, we use the opacity kernels

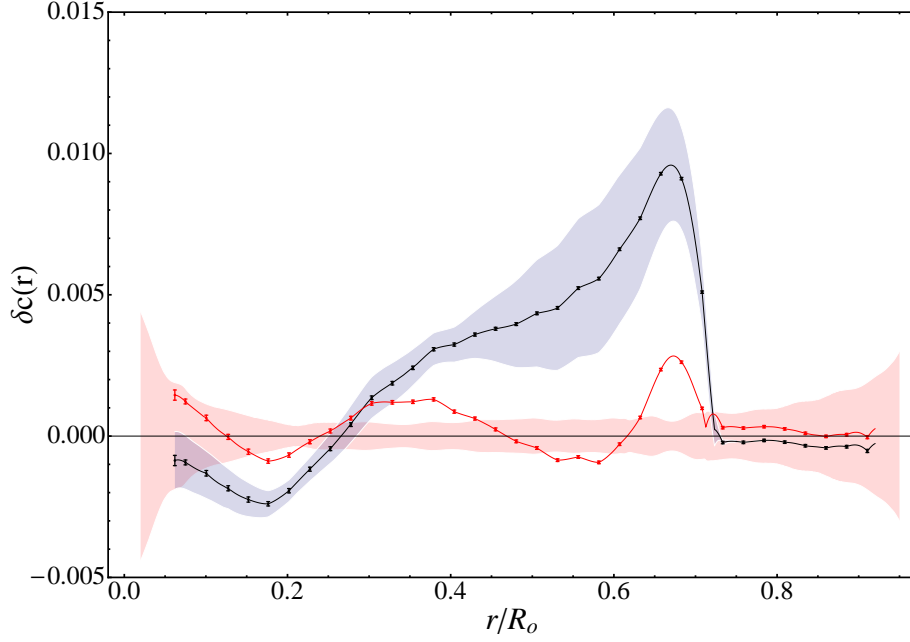


Fig. 1.— The fractional difference $\delta c_i \equiv (c_{\text{obs},i} - c(r_i)) / c(r_i)$ between the sound speed $c(r)$ predicted by SSMs and the values $c_{\text{obs},i}$ inferred from helioseismic data; the black line refers to the SSM model implementing the AGSS09 surface composition while the red line is obtained by using the GS98 admixture. The red band provides an estimate of the uncertainty in inversion of helioseismic data. The light blue band corresponds to the 1σ uncertainties in the theoretical predictions.

derived in Villante (2010) by adopting the linearization procedure proposed in Villante & Ricci (2010). The kernels $K_Q(r)$ represent the functional derivatives of the observable Q with respect to the opacity profile of the Sun and can be used to calculate the effects produced by an arbitrary opacity variation $\delta\kappa(r)$ according to:

$$\delta Q = \int dr K_Q(r) \delta\kappa(r) \quad (4)$$

where:

$$\delta Q \equiv \frac{Q}{\bar{Q}} - 1, \quad (5)$$

and

$$\delta\kappa(r) \equiv \frac{\kappa(\bar{T}(r), \bar{\rho}(r), \bar{Y}(r), \bar{Z}_j(r))}{\bar{\kappa}(\bar{T}(r), \bar{\rho}(r), \bar{Y}(r), \bar{Z}_j(r))} - 1 \quad (6)$$

In the above relation, the functions κ and $\bar{\kappa}$ are calculated along the density, temperature and chemical composition profiles predicted by SSM.

By using the kernels $K_Q(r)$, we propagate the uncertainty in the opacity profile of the Sun

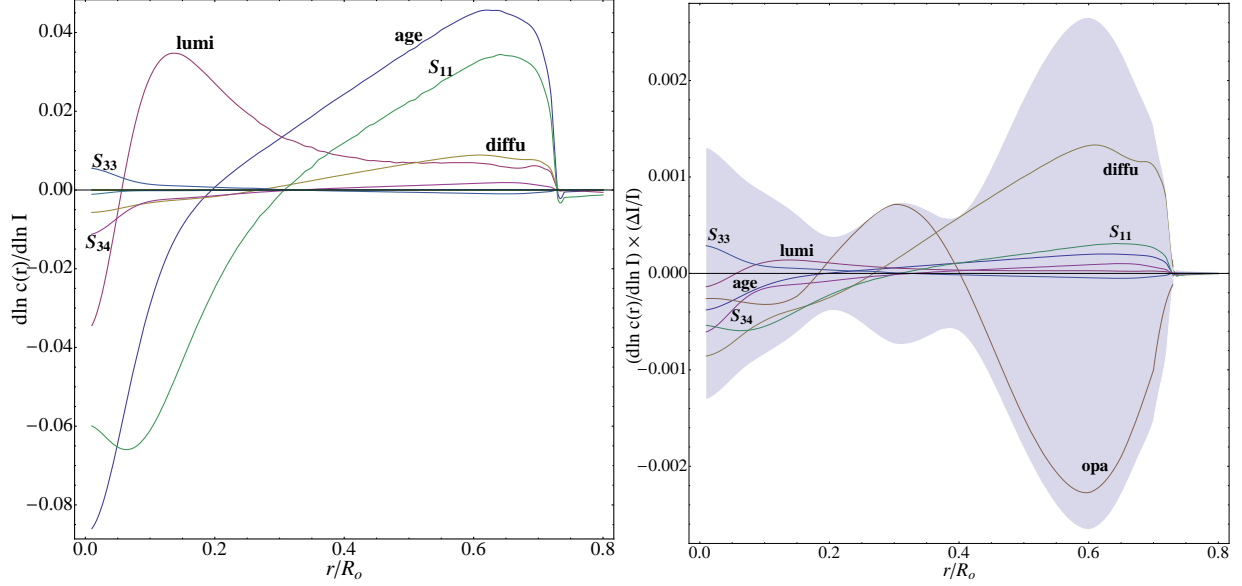


Fig. 2.— Left panel: The logarithmic derivatives of the sound speed profile defined in equation (2). Right panel: The contributions to uncertainties in the theoretical prediction of the sound speed profile defined in eqs.(3,7). The shaded area corresponds to the total theoretical error.

$\delta\kappa_{\text{opa}}(r)$ according to:

$$C_{Q,\text{opa}} \equiv \int dr K_Q(r) \delta\kappa_{\text{opa}}(r) \quad (7)$$

The standard prescription, adopted e.g. in Serenelli et al. (2009), is to consider a 2.5% global rescaling factor that corresponds to take $\delta\kappa_{\text{opa}}(r) \equiv 0.025$. However, this is not realistic because, albeit different groups typically provide opacity values that differ by $\sim \text{few}\%$ in the solar interior, there is a complicated dependence on the solar radius. Moreover, it was shown in Villante (2010) that the assumption of a global rescaling underestimates the uncertainties for the sound speed and for the depth of the convective envelope. The opacity kernels for these quantities are not positive definite and a constant $\delta\kappa$ produces effects in different regions of the Sun that partially compensate each other. For this reason, we take the difference between the OP (Badnell et al. 2005) and OPAL (Iglesias & Rogers 1996) tables as representative of uncertainties in opacity calculations, i.e. we assume

$$\delta\kappa_{\text{opa}}(r) \equiv \frac{\kappa_{\text{OPAL}}(\bar{T}(r), \bar{\rho}(r), \bar{Y}(r), \bar{Z}_i(r))}{\kappa_{\text{OP}}(\bar{T}(r), \bar{\rho}(r), \bar{Y}(r), \bar{Z}_i(r))} - 1 \quad (8)$$

The function $\delta\kappa_{\text{opa}}(r)$ is shown in Figure 3. The sound speed errors obtained with this assumption are much larger than what is obtained by the standard approach, even if $|\delta\kappa_{\text{opa}}(r)| \leq 0.025$ almost everywhere.

Finally, the total theoretical error for each observable Q is calculated by combining in quadra-

	Age	Diffu	Lum	S_{11}	S_{33}	S_{34}	S_{17}	S_{e7}	$S_{1,14}$	0pa
Y_b	-0.001	-0.012	0.002	0.001	0	0.001	0	0	0.	0.004
R_b	-0.0004	-0.0029	-0.0001	-0.0006	0.0001	-0.0002	0	0	0	0.0014
Φ_{pp}	0	-0.002	0.003	0.001	0.002	-0.003	0	0	0	-0.001
Φ_{Be}	0.003	0.022	0.014	-0.010	-0.023	0.047	0	0	0	0.009
Φ_B	0.006	0.044	0.029	-0.025	-0.022	0.046	0.075	-0.02	0	0.020
Φ_N	0.004	0.054	0.018	-0.019	0.001	-0.003	0	0	0.051	0.013
Φ_O	0.006	0.062	0.024	-0.027	0.001	-0.002	0	0	0.072	0.018

Table 3: The contributions $C_{Q,I}$ to uncertainties in theoretical predictions for helioseismic observables and solar neutrino fluxes.

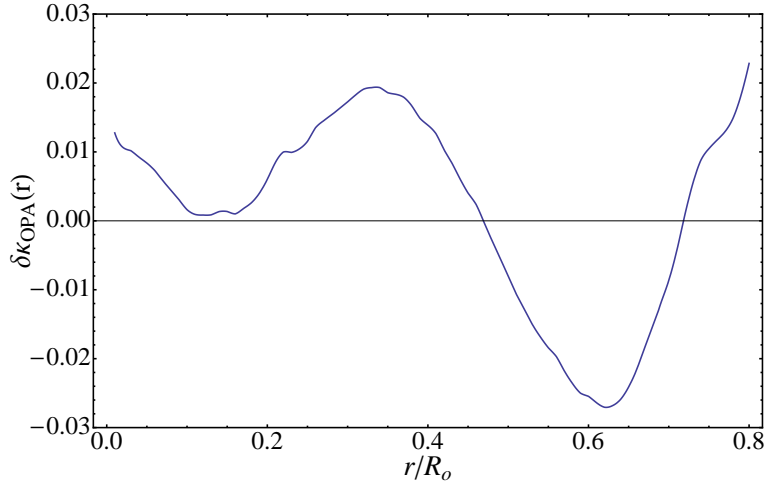


Fig. 3.— Fractional difference between OPAL and OP radiative opacities calculated along the SSM profile, see equation (8).

ture all the error contributions, i.e.

$$\sigma_{Q,\text{theo}}^2 = \sum_I C_{Q,I}^2 \quad (9)$$

where the sum extends over the 10 parameters listed in the beginning of this section.

2.3. Observational constraints

In the third column of Table 2, we give the observational values Q_{obs} for helioseismic and solar neutrino observables. The solar neutrino fluxes are obtained by performing a fit to all available solar neutrino data (Bellini et al. 2011). Among the various components, the ^8B and ^7Be neutrino fluxes are essentially determined by SK (Cravens et al. 2008) and SNO (Ahmad et al. 2002) and by Borexino (Arpesella et al. 2008) respectively, i.e. by two independent sets of experimental data.

We thus include the two values

$$\begin{aligned}\Phi_{\text{Be,obs}} &= 4.82 (1^{+0.05}_{-0.04}) \times 10^9 \text{cm}^{-2} \text{s}^{-1} \\ \Phi_{\text{B,obs}} &= 5.00 (1 \pm 0.03) \times 10^6 \text{cm}^{-2} \text{s}^{-1}.\end{aligned}\tag{10}$$

and assume their errors are uncorrelated. Generically denoting with U_Q an uncorrelated fractional error in the observable Q , we adopt

$$\begin{aligned}U_{\text{Be}} &= 0.045 \\ U_{\text{B}} &= 0.03\end{aligned}\tag{11}$$

for Φ_{Be} and Φ_{B} respectively. We note that the observational errors are smaller than the uncertainties in theoretical predictions.

The surface helium abundance and the inner radius of the convective envelope are obtained by inversion of helioseismic frequencies. We adopt the values

$$\begin{aligned}Y_{\text{b,obs}} &= 0.2485 \pm 0.0035 \\ R_{\text{b,obs}} &= 0.713 \pm 0.001\end{aligned}\tag{12}$$

which are obtained in Basu & Antia (2004) and Basu & Antia (1997) respectively, and we indicate with

$$\begin{aligned}U_Y &= 0.015 \\ U_R &= 0.0014\end{aligned}\tag{13}$$

the fractional errors that we assume, as it is usually done (see e.g. Delahaye & Pinsonneault 2006), not being significantly correlated.

The sound speed data points δc_i reported in Figure 1 have been obtained in Basu et al. (2009) with the set of frequencies of solar low-degree p modes from the BiSON network by using the Subtractive Optimally Localized Averages (SOLA) inversion technique. The various points are localized at the target radii r_i of the corresponding averaging kernels. The displayed error bars $U_{i,\text{exp}}$ are calculated by propagating the observational uncertainties of the measured frequencies. It is well known, however, that larger errors arise from the choice of the parameters in the inversion procedure and from the assumed starting model for the inversion. An extensive investigation of uncertainties in helioseismic determinations of sound speed has been performed in Degl’Innocenti et al. (1997)². The red band in Figure 1 corresponds to the so-called “statistical” uncertainty $U_{\text{stat}}(r)$ that is obtained in Degl’Innocenti et al. (1997) by combining in quadrature all the relevant

²Degl’Innocenti et al. (1997) adopted two different inversion methods, depending on the value of the radial coordinate. For $r/R_{\odot} \geq 0.1$, the Regularized Least Square (RLS) method was used. In the inner region, an hybrid method combining the SOLA and the RLS techniques was used.

error contributions. In our analysis, we define total (fractional) observational errors for the sound speed by combining in quadrature experimental and “statistical” errors according to:

$$U_{c,i} = \sqrt{U_{i,\text{exp}}^2 + U_{\text{stat}}^2(r_i)} \quad (14)$$

where the index i indicates the considered data point. Clearly, sound speed determinations at different radii are expected to have a certain degree of correlation because uncertainties are mainly related to the inversion procedure. Unfortunately, the information provided in the scientific literature does not allow us to quantify these correlations. For this reason, we include the sound speed errors as being uncorrelated. The correct quantification of helioseismic errors is an important ingredient and it would be desirable that the complete information were provided in future investigations.

As it is well known, solar models implementing the AGSS09 admixture do not correctly reproduce the helioseismic constraints. By combining in quadrature theoretical and observational errors, we see that the predictions for Y_{b} and R_{b} deviates from observational data at $\sim 3.6\sigma$ and $\sim 3.9\sigma$ respectively³. The sound speed at $r \sim 0.65 R_{\odot}$ differs from the results of helioseismic inversion by $\sim 4.6\sigma$. Helioseismic data are much better fitted by solar models implementing the GS98 surface composition, as it can be seen from Table 2 and Figure 1. A reasonable agreement exists between predicted and reconstructed solar neutrino fluxes both for the AGSS09 and the GS98 solar models.

3. The statistical approach

Our goal is to build a χ^2 function that can be used as a figure-of-merit for SSMs with different compositions. Let us consider a generic observable quantity with its associated observational value Q_{obs} and theoretical prediction Q . We indicate with

$$\delta Q_{\text{obs}} = \frac{Q_{\text{obs}}}{Q} - 1 \quad (15)$$

the fractional difference between the observational value and the theoretical result. In this work, we consider a set of $N = 34$ differences δQ given by

$$\{\delta Q_{\text{obs}}\} = \{\delta\Phi_{\text{B}}, \delta\Phi_{\text{Be}}, \delta Y_{\text{b}}, \delta R_{\text{b}}; \delta c_1, \delta c_2, \dots, \delta c_{30}\} \quad (16)$$

where we include the sound speed determinations $c_{i,\text{obs}}$ of Basu et al. (2009) that are localised at $r \leq 0.8R_{\odot}$.

The differences δQ_{obs} are affected by the uncorrelated errors U_Q (e.g. from neutrino experiments and helioseismic data) and by a set of systematic correlated errors $C_{Q,I}$ induced by $K = 10$

³These discrepancies are slightly different from what found by Bahcall et al. (2006). This is due to the fact that we use a different prescription for the opacity uncertainty; we do not include composition uncertainties in the error budget; Bahcall et al. (2006) use the surface composition of Asplund et al. (2005).

independent sources that, in our approach, are⁴

$$\{I\} = \{\text{opa; age; diffu; lum; } S_{11}, S_{33}, S_{34}, S_{17}, S_{e7}, S_{1,14}\} \quad (17)$$

Following Fogli et al. (2002), we define χ^2 as

$$\chi^2 = \min_{\{\xi_I\}} \left[\sum_Q \left(\frac{\delta Q_{\text{obs}} - \sum_I \xi_I C_{Q,I}}{U_Q} \right)^2 + \sum_I \xi_I^2 \right]. \quad (18)$$

This definition describes the effects of systematic correlated errors $C_{Q,I}$ by introducing the shifts $-\xi_I C_{Q,I}$, where ξ_I is a univariate gaussian random variable. Expressing χ^2 in this way is completely equivalent to the standard covariance matrix approach (for a formal proof refer to Fogli et al. 2002). However, it offers some relevant advantages: 1) it is more easily implemented numerically and; 2) it allows to trace the individual contributions to the χ^2 . Denoting with $\tilde{\xi}_I$ the values that minimize the χ^2 , one obtains

$$\chi^2 \equiv \chi_{\text{obs}}^2 + \chi_{\text{syst}}^2 = \sum_Q \tilde{X}_Q^2 + \sum_I \tilde{\xi}_I^2 \quad (19)$$

where

$$\tilde{X}_Q \equiv \frac{\delta Q_{\text{obs}} - \sum_I \tilde{\xi}_I C_{Q,I}}{U_Q} \quad (20)$$

are the so-called “pulls” of observational quantities. The values $\tilde{\xi}_I$ are instead referred to as the “pulls” of systematical error sources that, in our analysis, coincides with input parameters in solar model construction. The distribution of the $\tilde{\xi}_I$ can thus be used to highlight tensions in SSM assumptions. The optimal composition of Sun is found by minimizing the χ^2 and the obtained value χ_{min}^2 provides information on the goodness of the fit. The allowed regions are determined by cutting at prescribed values of the variable $\Delta\chi^2 \equiv \chi^2 - \chi_{\text{min}}^2$.

4. Describing the role of metals

We study the response of the Sun to changes in the heavy element admixture $\{z_j\}$, expressed in terms of the quantities

$$z_j \equiv Z_{j,b}/X_b \quad (21)$$

where $Z_{j,b}$ is the surface abundance of the j -element, X_b is that of hydrogen, and the index j runs over all relevant metals (see Table 4). We determine the dependence of the observables on

⁴In this work, correlated systematic errors incidentally coincide with theoretical uncertainties, while uncorrelated errors coincide with observational uncertainties. However, this is not necessarily the case. For example, were we to use Φ_{pp} as an observable in our analysis, there would exist a correlation between its experimental error and that of Φ_{Be} due to the *luminosity constraint* usually adopted in the analysis of solar neutrino data, see e.g. Gonzalez-Garcia et al. (2010).

	C	N	O	Ne	Mg	Si	S	Fe	CNO	Met
Y_b	-0.003	0.001	0.025	0.030	0.032	0.063	0.043	0.086	0.023	0.223
R_b	-0.005	-0.003	-0.027	-0.011	-0.004	0.002	0.004	-0.009	-0.035	-0.007
Φ_{pp}	-0.005	-0.001	-0.004	-0.004	-0.004	-0.008	-0.006	-0.017	-0.010	-0.034
Φ_{Be}	0.004	0.002	0.052	0.046	0.048	0.103	0.073	0.204	0.058	0.429
Φ_B	0.026	0.007	0.112	0.088	0.089	0.191	0.134	0.501	0.145	0.916
Φ_N	0.874	0.147	0.057	0.042	0.044	0.102	0.072	0.263	1.078	0.480
Φ_O	0.827	0.206	0.084	0.062	0.065	0.145	0.102	0.382	1.117	0.694

Table 4: The logarithmic derivatives $\mathcal{B}_{Q,j} = d \ln Q / d \ln z_j$ with respect to the surface abundances.

the surface composition by constructing solar models in which each z_j is varied individually. We observe that the effects produced by a change of composition $\{\delta z_j\}$ are well described by a linear relation

$$\delta Q = \sum_j \mathcal{B}_{Q,j} \delta z_j, \quad (22)$$

where δz_j is the fractional variations of z_j

$$\delta z_j \equiv \frac{z_j}{\bar{z}_j} - 1 \quad (23)$$

with respect to the AGSS09 value \bar{z}_j . In this assumption, the coefficients $\mathcal{B}_{Q,i}$ represent the logarithmic derivatives of Q with respect to the j -element surface abundance, i.e.

$$\mathcal{B}_{Q,j} = \frac{d \ln Q}{d \ln z_j}. \quad (24)$$

The values obtained for the $\mathcal{B}_{Q,j}$ coefficients are reported in Table 4. Our results can be compared with the coefficients presented in Serenelli et al. (2009). The small differences arise from the fact that we considered relatively large variations for the various abundances, in order to check the adequacy of rel. (22) over the ranges of compositions required by our analysis. The logarithmic derivative $\mathcal{B}_{c,j}(r)$ of the sound speed with respect to the surface composition have not been shown elsewhere in scientific literature and are given in the left panel of Figure 4.

The accuracy of equation (22) can be tested by using it to reproduce the predictions of the GS98 solar model starting from those obtained by implementing the AGSS09 surface composition. The results of this exercise, the *reconstructed* GS98 (GS98rec) model, are shown in the last column of Table 2 and in Figure 5. The differences between GS98 and AGSS09 are reproduced with $\sim 20\%$ accuracy (in the worst cases) and the errors introduced by the use of the linear approximation are always smaller or comparable to theoretical and observational uncertainties. The use of relation (22) greatly simplifies the numerical problem of scanning over the range of possible compositions. In this assumption, indeed, the χ^2 is expressed as a quadratic function of the various δz_j that can be

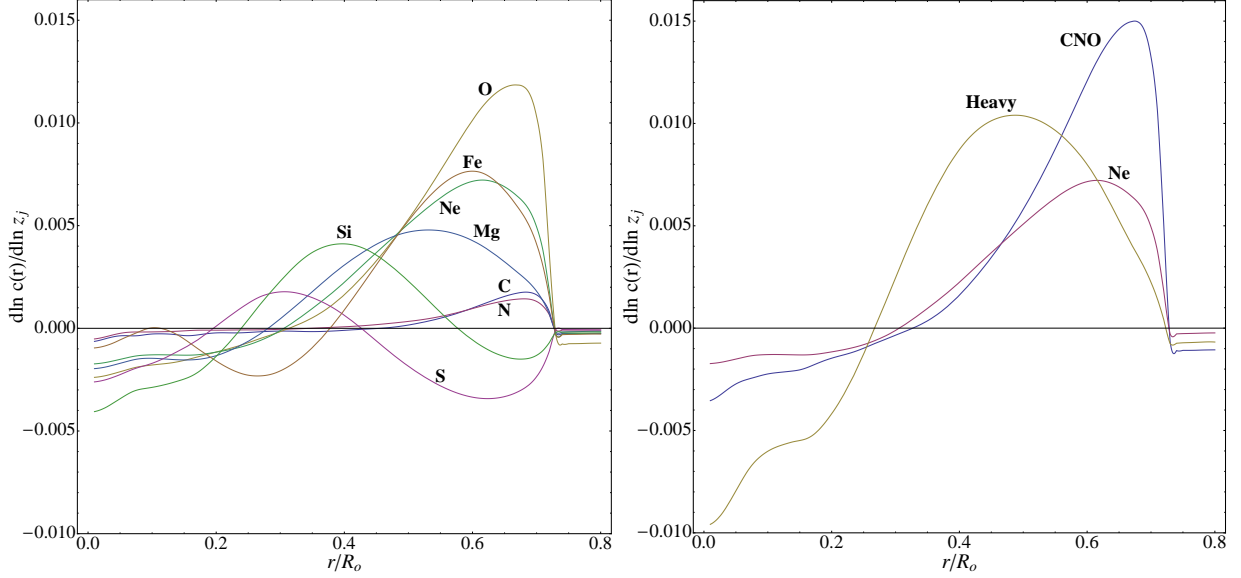


Fig. 4.— Left panel: Logarithmic derivatives of the sound speed with respect to the surface abundances z_j . Right Panel: Logarithmic derivatives of the sound speed with respect to the total CNO, Ne and *meteoritic* elements surface abundances.

effectively minimized. We obtain

$$\chi^2 = \min_{\{\xi_I\}} \left[\sum_Q \left(\frac{\delta \bar{Q} - \sum_j \delta z_j B_{Q,j} - \sum_I \xi_I C_{Q,I}}{U_Q} \right)^2 + \sum_I \xi_I^2 \right]. \quad (25)$$

where

$$\delta \bar{Q} = \frac{Q_{\text{obs}}}{\bar{Q}} - 1 \quad (26)$$

is the fractional difference between the observational value Q_{obs} and the value \bar{Q} predicted by the AGSS09 solar model. Even with this simplification, however, it is not possible (nor useful) to consider all the δz_j as free parameters. For this reason, we group metals according to the method by which their abundances are determined. Following Delahaye et al. (2010), we consider three different groups given by (C + N + O), Ne, (Mg + Si + S + Fe) which include elements whose abundances are determined in the photosphere, in the chromosphere and corona, and in the meteorites, respectively. Within each group, we vary the elemental abundances according to same multiplicative factor. In other words, we define three independent parameters ($\delta z_{\text{CNO}}, \delta z_{\text{Ne}}, \delta z_{\text{met}}$) as

$$\begin{aligned} 1 + \delta z_{\text{CNO}} &\equiv \frac{z_{\text{C}}}{\bar{z}_{\text{C}}} \equiv \frac{z_{\text{N}}}{\bar{z}_{\text{N}}} \equiv \frac{z_{\text{O}}}{\bar{z}_{\text{O}}} \\ 1 + \delta z_{\text{Ne}} &\equiv \frac{z_{\text{Ne}}}{\bar{z}_{\text{Ne}}} \\ 1 + \delta z_{\text{met}} &\equiv \frac{z_{\text{Mg}}}{\bar{z}_{\text{Mg}}} \equiv \frac{z_{\text{Si}}}{\bar{z}_{\text{Si}}} \equiv \frac{z_{\text{S}}}{\bar{z}_{\text{S}}} \equiv \frac{z_{\text{Fe}}}{\bar{z}_{\text{Fe}}} \end{aligned}$$

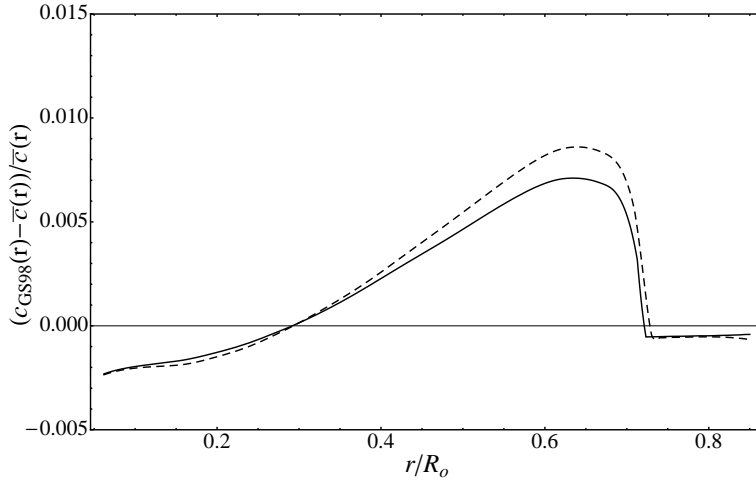


Fig. 5.— The solid line shows the fractional difference between the sound speed predicted by SSMs implementing GS98 admixture and that obtained by using AGSS09 surface compositions. The dashed line is obtained by using the linear expansion given by equation (22).

Based on this assumption and the linear relation (22), the logarithmic derivatives $\mathcal{B}_{Q,\text{CNO}}(r)$ and $\mathcal{B}_{Q,\text{met}}(r)$ of the various observables Q with respect to δz_{CNO} and δz_{met} are

$$\begin{aligned}\mathcal{B}_{Q,\text{CNO}} &\equiv \mathcal{B}_{Q,\text{C}} + \mathcal{B}_{Q,\text{N}} + \mathcal{B}_{Q,\text{O}} \\ \mathcal{B}_{Q,\text{met}} &\equiv \mathcal{B}_{Q,\text{Mg}} + \mathcal{B}_{Q,\text{Si}} + \mathcal{B}_{Q,\text{S}} + \mathcal{B}_{Q,\text{Fe}}\end{aligned}$$

and are reported in Table 4. The functions $\mathcal{B}_{c,\text{CNO}}(r)$, $\mathcal{B}_{c,\text{Ne}}(r)$ and $\mathcal{B}_{c,\text{met}}(r)$ describing the effects of each group of elements on the sound speed profile of the Sun are shown in the right panel of Figure 4.

5. Inferring the solar composition

5.1. Volatiles and refractories: a two-parameter analysis

As a first application, we consider a scenario in which the neon-to-oxygen ratio is fixed to the value prescribed by the AGSS09 compilation, i.e. we further constrain the possible variations of the heavy element admixture by assuming $\delta z_{\text{CNO}} = \delta z_{\text{Ne}}$. In this hypothesis, the χ^2 is defined in terms of two independent parameters $(\delta z_{\text{CNO}}, \delta z_{\text{met}})$ that are varied to fit helioseismic and solar neutrino constraints. A similar exercise was performed in Delahaye & Pinsonneault (2006) where, however, only the determinations of the surface helium abundance and of the convective radius were considered. Here, we include the information provided by the sound speed profile and the neutrino fluxes in a global quantitative analysis. The redundancy of the different pieces of experimental information allows us to obtain more solid constraints on the solar composition and, even more

relevant, to verify that a coherent picture emerge from the data and/or to highlight tensions in SSM assumptions.

Our results are presented in Figure 6 where we use the astronomical scale for logarithmic abundances ε_j in order to facilitate the comparison with observational data. The conversion from δz_j to ε_j is obtained by using the relation

$$\varepsilon_j = \bar{\varepsilon}_j + \log(1 + \delta z_j) \quad (27)$$

with the AGSS09 abundances $\bar{\varepsilon}_j$ given in Table 1. The coloured lines are obtained by cutting at $\Delta\chi^2 \equiv \chi^2 - \chi^2_{\min} = 2.3, 6.2, 11.8$ that correspond to 1, 2, 3 σ confidence levels for a χ^2 variable with 2 d.o.f.. The data points show the observational values for the oxygen and iron abundances in the AGSS09 and GS98 compilations. In order to show how different observational information combine in determining the optimal composition, we present separately the bounds obtained by using the: the helioseismic constraints on the surface helium abundance and the convective radius (upper-left panel); the ${}^7\text{Be}$ and ${}^8\text{B}$ neutrino flux determinations (upper-right panel); the 30 sound speed data points $c_{i,\text{obs}}$ from Basu et al. (2009) that are localized at $r \leq 0.8 R_\odot$ (lower-left panel); all the observational data simultaneously (lower-right panel). The main conclusions of our analysis are discussed in the following

- 1) The SSM implementing AGSS09 composition is excluded at a high confidence being $\chi^2/\text{d.o.f.} = 176.7/32$ when all the available observational constraints are considered. This result essentially arises from helioseismic observables that are in severe disagreement with AGSS09 predictions. The ${}^7\text{Be}$ and ${}^8\text{B}$ solar neutrino flux determinations do not discriminate among different compositions with the sufficient level of accuracy. This is mainly due to theoretical uncertainties which are dominated by the contributions from S_{34} and S_{17} , respectively, but also to a very mild dependence on CNO abundances.
- 2) There is a reasonable agreement between the information provided by the various observational constraints, as it can be seen by comparing the different panels of Figure 6. The best fit to the observational data is obtained for:

$$\begin{aligned} \delta z_{\text{CNO}} &= \delta z_{\text{Ne}} = 0.45 \pm 0.04 \\ \delta z_{\text{met}} &= 0.19 \pm 0.03 \end{aligned} \quad (28)$$

that correspond to $\varepsilon_{\text{O}} = 8.85 \pm 0.01$ and $\varepsilon_{\text{Fe}} = 7.52 \pm 0.01$. These values are consistent at $\sim 1\sigma$ level with those quoted in the GS98 compilation. They are close to the results of Delahaye & Pinsonneault (2006) but have considerably smaller uncertainties. The quality of the fit is quite good being the $\chi^2_{\min}/\text{d.o.f.} = 39.6/32$ when all the observational constraints are considered. The errors on the inferred abundances ε_{O} and ε_{Fe} are smaller than what is obtained by observational determinations. One caveat is, however, that we are considering a simplified scenario in which different elemental abundances are grouped together and forced to vary by the same multiplicative factors.

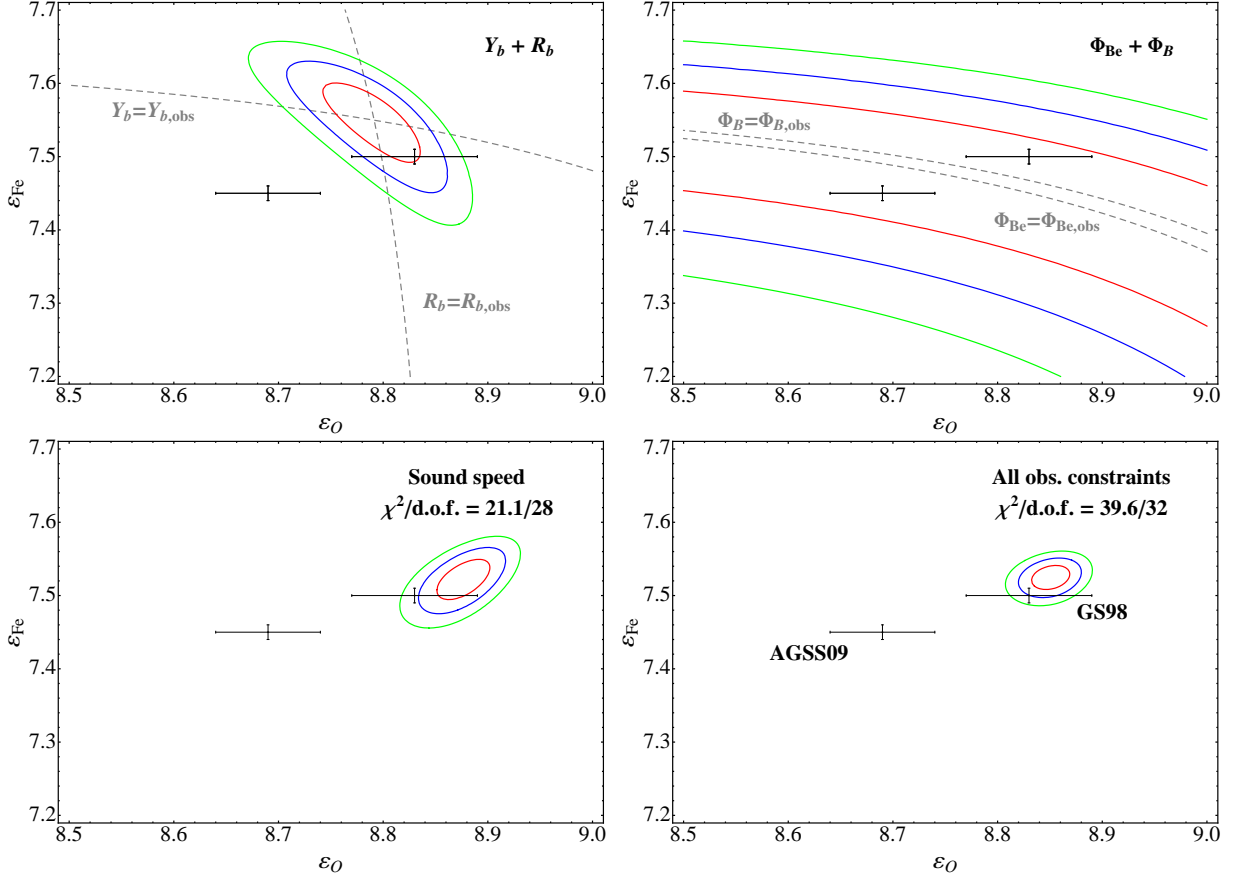


Fig. 6.— The bounds on ε_O and ε_{Fe} that are obtained from observational constraints. See text for details.

- 3) The observational and systematic contribution to χ^2_{min} are given by $\chi^2_{obs} = 35.1$ and $\chi^2_{syst} = 4.5$ respectively, with the distribution of systematic pulls $\tilde{\xi}_I$ at the best fit point reported in Table 5. The effects of systematic pulls (that correspond to correlated error sources) are relevant and cannot be neglected. This is seen e.g. in the upper-left panel of Figure 6 where we see that the error ellipse axes do not coincide with the lines $Y_b = Y_{b,obs}$ and $R_b = R_{b,obs}$, as it would be expected if error correlations were negligible. It is also evident from the red dots and the red line in Figure 7 that show the predictions Q of solar models implementing the best fit composition calculated by using the linear expansion (22). These predictions deviate from the observational constraints by amounts that are larger than the uncorrelated observational errors. However, this does not imply that the quality of the fit is bad since one has the possibility to change the SSM inputs within their range of uncertainty as it is

	Opac	Age	Lum	Diffu	S_{11}	S_{33}	S_{34}	S_{e7}	S_{17}	$S_{1,14}$
$\tilde{\xi}_I$	1.07	0.03	-0.41	-0.74	~ 0	0.46	-0.97	0.32	-1.20	~ 0
$\tilde{\xi}_I \delta I$	$1.07 (\kappa_{\text{OPAL}}/\kappa_{\text{OP}} - 1)$	~ 0	-0.0016	-0.11	~ 0	0.024	-0.05	0.007	-0.09	~ 0

Table 5: The pulls of systematics $\tilde{\xi}_I$ at the best fit point and the fractional variations $\tilde{\xi}_I \delta I$ of the corresponding input parameters. All the available observational information are simultaneously fitted. The entries with ~ 0 are smaller (in magnitude) than 10^{-2} in the first line and 10^{-3} in the second line.

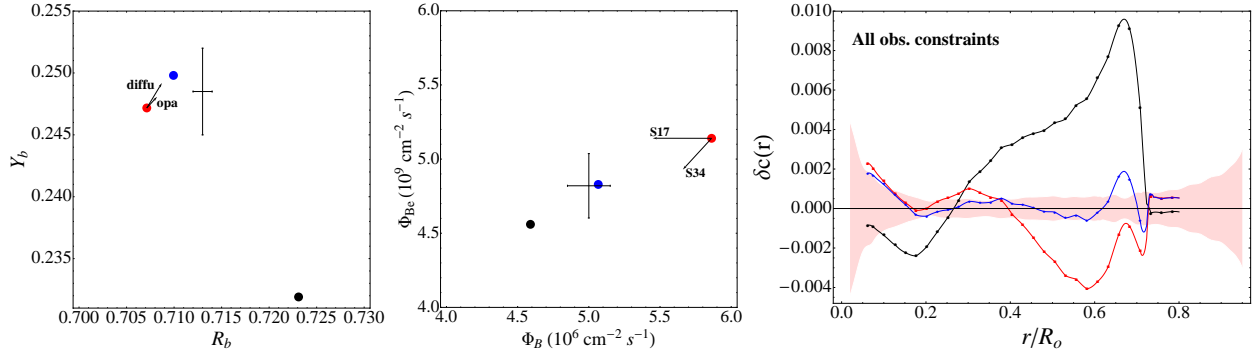


Fig. 7.— The helioseismic and solar neutrino observables predicted by AGSS09 solar model (black) and by the solar model providing the best fit to all observational constraints with (blue) and without (red) taking into account the pulls of systematical errors.

described in equation (25). The blue dots and the blue line in Figure 7 show the quantities

$$\tilde{Q} = Q \left[1 + \sum_I C_{Q,I} \tilde{\xi}_I \right] \quad (29)$$

that include the effects due to the pulls of systematic errors. The quantities \tilde{Q} differ quite substantially from the corresponding Q and agree quite well with the observational constraints. The dominant contributions to systematic shifts are shown by the black arrows in Fig. 7 and are provided by: opacity for the sound speed $c(r)$ (see discussion in the next paragraph); diffusion coefficients which are decreased by $\sim 11\%$ in order to improve consistency between Y_b and R_b and the sound speed profile $c(r)$; the astrophysical factors S_{34} and S_{17} that are decreased by $\sim 5\%$ and $\sim 9\%$ respectively in order to improve agreement with Φ_B and Φ_{Be} measurements.

- 4) The large systematic shift of the sound speed due to opacities, $\tilde{\xi}_{\text{opa}} = 1.07$, indicates that there is tension between observational data and SSMs implementing OP opacity tables. Indeed, if we restrict our analysis to OP opacities, i.e. we choose $\xi_{\text{opa}} \equiv 0$ in our approach, the quality of the fit is considerably decreased. The best fit is obtained for $\delta z_{\text{CNO}} = 0.33 \pm 0.03$

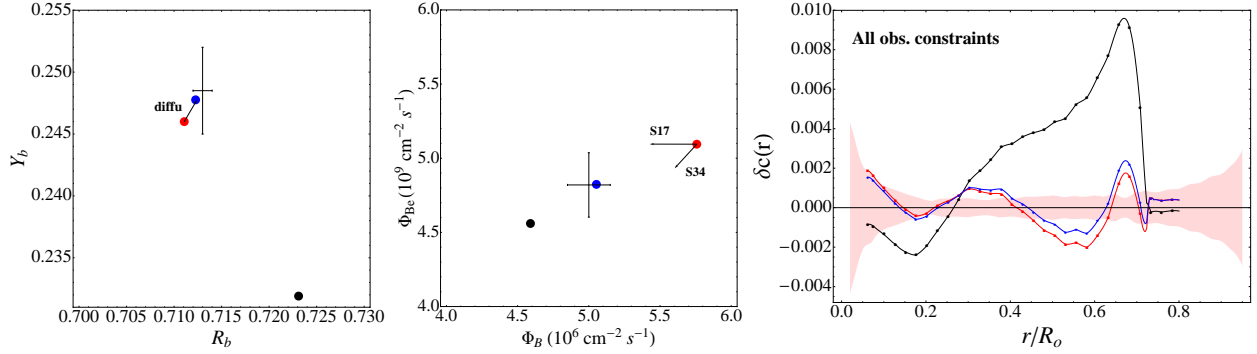


Fig. 8.— Same as Figure 7 but assuming $\xi_{\text{opa}} \equiv 0$.

and $\delta z_{\text{met}} = 0.19 \pm 0.03$ with $\chi^2_{\text{min}}/\text{d.o.f.} = 66.9/32$ when all observational constraints are considered. Solar models implementing OP opacities are disfavoured because they provide a less satisfactory fit of the sound speed in the region $0.3 < r/R_{\odot} < 0.6$, as it can be seen from Figure 8. It is interesting to note that, when ξ_{opa} is allowed to vary, the best fit is obtained with $\tilde{\xi}_{\text{opa}} \sim 1$ which means that observational data are better described when using OPAL opacity tables⁵. The statistical significance of this indication relies on the correct evaluation of the sound speed error in the outer radiative region of the Sun and may be weakened (or strengthened) by the possibility of correlations in the inferences of the solar sound speed at different target radii (not considered here due to lack of the necessary information in the scientific literature).

- 5) The CNO neutrino fluxes are expected to be $\sim 50\%$ larger than those predicted by SSMs implementing AGSS09 composition. Indeed, solar models providing a good fit to the observational data give $\Phi_N \simeq 3.4 \times 10^8 \text{ cm}^{-2} \text{ s}^{-1}$ and $\Phi_O \simeq 2.5 \times 10^8 \text{ cm}^{-2} \text{ s}^{-1}$ as a combined effect of the changes in composition and, to a minor extent, of the systematic shifts in the input parameters. These values are even larger than predictions obtained by assuming GS98 surface composition. However, this result depends on the assumed heavy element grouping. The CNO neutrino fluxes, in fact, are essentially determined by the carbon abundance, see Table 4, while the observational data included in our analysis are basically sensitive to the oxygen content of the Sun, since this element provides a large contribution to the solar opacity.

⁵We remind that we used the fractional difference between OPAL and OP opacities to define the opacity profile uncertainty $\delta \kappa_{\text{opa}}(r)$, see eq. (8).

5.2. Three-parameter analysis

It is important to discuss how the above results changes when the neon-to-oxygen ratio is allowed to vary, since Ne lacks photospheric features and the Ne/O ratio has to be inferred indirectly from solar wind measurements. In this assumption, the χ^2 is described as a function of three parameters ($\delta z_{\text{CNO}}, \delta z_{\text{Ne}}, \delta z_{\text{met}}$) that can be adjusted independently to reproduce helioseismic and solar neutrino constraints. In order to prevent unphysical results, we add a penalty function to the χ^2 given by:

$$\chi_{\text{pen}}^2 = \left[\frac{\delta z_{\text{Ne}} - \delta z_{\text{CNO}}}{\Delta (1 + \delta z_{\text{CNO}})} \right]^2 \quad (30)$$

where $\Delta = 0.3$, that forces the neon-to-oxygen ratio to the value prescribed by AGSS09 compilation with a 1σ accuracy equal to 30%, as it has been observed by Bahcall et al. (2005). The bounds obtained by considering all the available observational constraints are shown in Figure 9. The best fit composition is:

$$\begin{aligned} \delta z_{\text{CNO}} &= 0.37 \pm 0.07 \\ \delta z_{\text{Ne}} &= 0.80 \pm 0.26 \\ \delta z_{\text{met}} &= 0.13 \pm 0.05 \end{aligned} \quad (31)$$

that correspond to $\varepsilon_{\text{O}} = 8.83 \pm 0.02$, $\varepsilon_{\text{Ne}} = 8.19 \pm 0.06$ and $\varepsilon_{\text{Fe}} = 7.50 \pm 0.02$. These values are still consistent at $\sim 1\sigma$ with those obtained in the GS98 compilation. However, the errors in the inferred abundances are larger than before. We note, in particular, that the neon abundance is bounded at the level of accuracy prescribed by the function (30) indicating that the observational data are not effective in constraining it. The neon-to-oxygen ratio is increased by about $\sim 30\%$ with respect to the AGSS09 value. The quality of the fit, however, is not significantly improved being $\chi_{\text{min}}^2/\text{d.o.f.} = 37.8/31$ and the assumption $1 + \delta z_{\text{Ne}} = 1 + \delta z_{\text{CNO}}$ is allowed at 1σ .

The consequence of leaving neon as a free parameter is to introduce degeneracies between the various δz_j , as it is understood from inspection of Figure 9 and, in particular, by comparison of the left panel in Figure 9 and the lower-left panel of Figure 6. It exists, in fact, a combination of $\delta z_{\text{CNO}}, \delta z_{\text{Ne}}$ and δz_{met} that, taking also into account the effects of systematic pulls ξ_I , leaves substantially unchanged the observational properties of the Sun. An increase of neon-to-oxygen ratio can be compensated by a slight reduction of CNO and/or Heavy elements according to simple approximate formula:

$$\begin{aligned} \delta z_{\text{CNO}} &= 0.45 - 0.19 \Delta_{\text{CNO}}^{\text{Ne}} \\ \delta z_{\text{met}} &= 0.19 - 0.14 \Delta_{\text{CNO}}^{\text{Ne}} \end{aligned} \quad (32)$$

where $\Delta_{\text{CNO}}^{\text{Ne}} = \delta z_{\text{Ne}} - \delta z_{\text{CNO}}$, together with a re-adjustment of the systematic pulls:⁶

$$\tilde{\xi}_{\text{opa}} = 1.07 + 0.76 \Delta_{\text{CNO}}^{\text{Ne}}$$

⁶ For simplicity, we report here only the systematic pulls that are sensitive the neon-to-oxygen ratio.

$$\begin{aligned}
\tilde{\xi}_{\text{diffu}} &= -0.74 - 0.41 \Delta_{\text{CNO}}^{\text{Ne}} \\
\tilde{\xi}_{\text{s33}} &= 0.46 - 0.28 \Delta_{\text{CNO}}^{\text{Ne}} \\
\tilde{\xi}_{\text{s34}} &= -0.97 + 0.58 \Delta_{\text{CNO}}^{\text{Ne}} \\
\tilde{\xi}_{\text{s17}} &= -1.20 + 0.62 \Delta_{\text{CNO}}^{\text{Ne}}
\end{aligned} \tag{33}$$

From the above relations, we see that a 30% uncertainty in the neon-to-oxygen ratio roughly corresponds to $\sim 6\%$ and $\sim 4\%$ errors in the inferred CNO and heavy element abundances.

This degeneracy can be discussed at a more basic level by considering that the main effect produced by a change of the solar composition is the modification of the opacity profile of the Sun. The source term $\delta\kappa(r)$ that drives the modification of the solar properties and that is probed by observational data can be written as the sum of two contributions (Villante 2010) :

$$\delta\kappa(r) = \delta\kappa_{\text{I}}(r) + \delta\kappa_{\text{Z}}(r) \tag{34}$$

The *intrinsic* opacity change, $\delta\kappa_{\text{I}}(r)$, represents the fractional variation of the opacity along the SSM profile and it is given, in our approach, by $\delta\kappa_{\text{I}}(r) = \tilde{\xi}_{\text{opa}} \delta\kappa_{\text{opa}}(r)$. The *composition* opacity change $\delta\kappa_{\text{Z}}(r)$ can be approximately calculated as:

$$\delta\kappa_{\text{Z}}(r) \simeq \sum_j \frac{\partial \ln \kappa(r)}{\partial \ln Z_j} \delta z_j \tag{35}$$

by using the logarithmic derivatives $\partial \ln \kappa / \partial \ln Z_j$ that are presented in the left panel of Figure 10. Taking advantage of rel. (34), we calculate the effective opacity change $\delta\kappa(r)$ that corresponds to the models that provide a good fit to observational data. We see that $\delta\kappa(r)$ is well constrained by the available observational information. Opacity should be increased by $\sim \text{few}\%$ at the center of the Sun and by $\sim 25\%$ at the bottom of the convective envelope, as it was calculated by Villante (2010). The moderate increase at the solar center improves the agreement with $Y_{\text{b,obs}}$ without affecting the solar neutrino fluxes. The increasing trend of $\delta\kappa(r)$ is required to fit the convective radius R_{b} and sound speed profile δc_1 (see Villante (2010)). The wavy behaviour at intermediate radii improves consistency with inferred sound speed values in the region $0.3 < r/R_{\odot} < 0.6$. The general features of $\delta\kappa(r)$ are essentially independent on the assumptions about the opacity uncertainty. In this respects, the increase of the CNO and/or Ne content is interpreted as providing the “tilt” to $\delta\kappa(r)$, and is a solid conclusion of our analysis.

Figure 10, right panel, also compares the effective variations of opacity $\delta\kappa(r)$ obtained in the two and three parameter analysis. In particular, the black dashed line corresponds to the solar model with the composition given by equation (31) and the value $\tilde{\xi}_{\text{opa}} = 1.40$ calculated from equation (33). The red dotted line represents the effective opacity variation obtained with parameters given by equation (28) and $\tilde{\xi}_{\text{opa}} = 1.07$. We see that the two lines coincide at the 2% level or better. From this, we infer that the reconstructed opacity profile does not depend on the assumed heavy element grouping. Moreover, we understand that the compositions (28) and (31) cannot be discriminated by the adopted observational constraints. More in general, they cannot

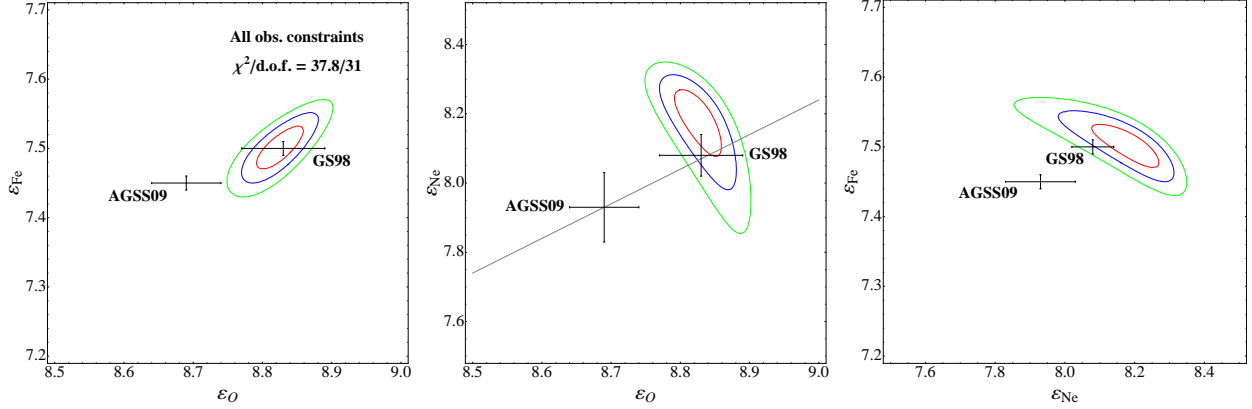


Fig. 9.— The bounds on ε_O , ε_{Ne} and ε_{Fe} that are obtained by considering all the available observational constraints. The gray line in the middle panel corresponds to the condition $\delta z_{Ne} = \delta z_{CNO}$, i.e. to the neon-to-oxygen ratio prescribed by AGSS09 compilation.

be distinguished by any conceivable observational test that is dominated by the opacity profile in the radiative region of the Sun: the 2% difference is indeed smaller than the accuracy to which the opacity of the solar plasma is known. In summary, the neon-to-oxygen ratio cannot be effectively constrained with current data.

6. Conclusions and perspectives

In this work, we have investigated the properties of the Sun by using a statistical approach, normally adopted in other area of physics, in which the information provided by solar neutrino and helioseismic data can be combined in a quantitative and effective way. Namely, we have inferred the chemical composition of the Sun by using the helioseismic determinations of the surface helium abundance and of the depth of the convective envelope; the measurements of 7Be and 8B neutrino fluxes; the solar sound speed profile inferred from helioseismic frequencies.

A consistent picture emerges from the combination of the different pieces of observational information which can be summarized as discussed in the following.

- i)* The surface composition prescribed by AGSS09 is excluded at an high confidence level, being the $\chi^2/d.o.f. = 176.7/32$ when all observational constraints are considered, unless the SSM's chemical evolution paradigm is not correct and/or the opacity calculations are wrong;
- ii)* A satisfactory fit to the available observational data ($\chi^2/d.o.f. = 39.6/32$) is obtained in the context of a two parameter analysis in which volatile (i.e. C, N, O and Ne) and refractory elements (i.e. Mg, Si, S and Fe) are grouped together and forced to vary by the same multiplicative factors. The abundance of volatile elements should be increased by $(45 \pm 4)\%$ while that of refractory elements should be increased by $(19 \pm 3)\%$ with respect to AGSS09 values;

iii) If the neon-to-oxygen ratio is allowed to vary within the currently allowed range (i.e. $\pm 30\%$ at 1σ), the best fit composition is obtained by increasing by $(37 \pm 7)\%$ the CNO elements; by $(80 \pm 26)\%$ the neon; by $(13 \pm 5)\%$ the refractory elements. The quality of the fit is, however, not significantly improved with respect to the two parameter analysis, being $\chi^2/\text{d.o.f.} = 37.8/31$.

By taking advantage of the adopted statistical approach, we were able to obtain few additional conclusions concerning the properties of the Sun which are discussed in the following.

iv) Under the two and three parameter analyses, the CNO neutrino fluxes are expected to be substantially larger than those predicted by SSM implementing the AGSS09 surface composition, although the exact value cannot be predicted in a model independent way since it depends on the assumed heavy elements grouping. In particular, this stems from assuming a the same fractional variation between C, N and O, a constraint that should be lifted when CNO neutrino fluxes are finally determined experimentally;

v) The sound speed in the region $0.3 < r/R_\odot < 0.6$ is better fitted by using the old OPAL opacity tables rather than the more recent OP opacity table. Indeed, when we restrict our analysis to OP opacities, the quality of the fit is considerably decreased giving $\chi^2/\text{d.o.f.} = 66.9/32$;

vi) The observational data prefer values for the input parameters of the standard solar models that are slightly different from those presently adopted. Namely, the best fit is obtained by decreasing the diffusion coefficients by $\sim 10\%$ and the astrophysical factors S_{34} and S_{17} are decreased by $\sim 5\%$ and $\sim 9\%$ respectively, when all observational constraints are considered.

The above results are obtained by using a simplified approach in which elements are lumped together in two or three groups and they essentially follow from the fact that the opacity profile of the solar radiative region is well constrained by the combination of the different observational data, as it is shown by the gray band in the right panel of in Figure 10. A substantial improvement with respect to the present situation could be provided by observational constraints where the degeneracy between opacities and composition is lifted. One such constraint has already explored before and is linked to the sensitivity of the acoustic p-modes to the adiabatic index $\Gamma_1 = \frac{\partial P}{\partial \rho_{\text{ad}}}$. Results available in the literature are contradictory. Lin et al. (2007) concludes the metallicity of the solar envelope is comparable to that of GS98. However, using different techniques for constructing the solar envelope models and the inversion procedures, and also a different equation of state, Vorontsov et al. (2013) find a solar metallicity that is even lower than AGSS09 values. It is important to mention that $\Gamma_1 = \frac{\partial P}{\partial \rho_{\text{ad}}}$, while independent of radiative opacities, depends crucially on the details of the equation of state. A second possibility is offered by the neutrino fluxes from the CN-cycle. While a detailed quantitative analysis will be presented elsewhere (Villante & Serenelli 2013), it is important to stress at least qualitatively the importance of a CNO neutrino measurement. Even a low accuracy measurement, providing a direct determination of the metallicity of the solar core, permits to remove the degeneracy between opacity and composition effects. Let us imagine e.g. to measure the CNO flux at the 20% level. If the detected fluxes were consistent with the expectations from our analysis (i.e. about 50% larger than the reference predictions), this would be sufficient to conclude that the AGSS09 surface abundances are wrong and/or the chemical evolution paradigm

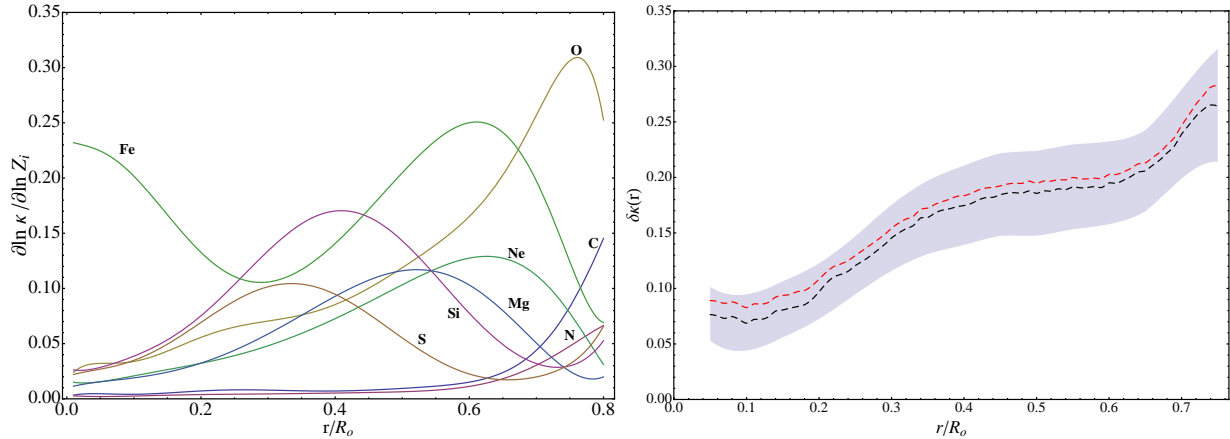


Fig. 10.— Left panel: The logarithmic derivatives of opacity with respect to individual metal abundances calculated along the SSM profile. Right panel: The effective opacity change $\delta \kappa(r)$ of solar models that provide a good fit to observational constraints when $(\delta z_{\text{CNO}}, \delta z_{\text{Ne}}, \delta z_{\text{met}})$ are allowed to vary. The black dashed line correspond to the best fit model. The red dashed line correspond to the best fit model obtained with the additional assumption that $\delta Z_{\text{Ne}} = \delta z_{\text{CNO}}$, i.e. that the neon-to-oxygen ratio is equal to the value prescribed by AGSS09 compilation.

of the SSM is not correct. There would be no possibility to explain the observed results by assuming that opacity (or, more in general energy transport in the Sun) is not correctly described. On the contrary, if the detected fluxes were consistent with those predicted by solar models using AGSS09 admixture, then this would imply a tension with other observational constraints. This tension could be only explained by assuming that opacity calculations are wrong by a factor much larger than the presently estimated uncertainties. Both these results would have enormous implications for stellar evolution.

A.S. is supported by the MICINN grant AYA2011-24704 and by the ESF EUROCORES Program EuroGENESIS (MICINN grant EUI2009-04170).

REFERENCES

- Abdurashitov, J. N., Bowles, T. J., Cherry, M. L., et al. 1999, *Physical Review Letters*, 83, 4686
- Adelberger, E. G., García, A., Robertson, R. G. H., et al. 2011, *Reviews of Modern Physics*, 83, 195
- Ahmad, Q. R., Allen, R. C., Andersen, T. C., et al. 2001, *Physical Review Letters*, 87, 071301
- . 2002, *Physical Review Letters*, 89, 011301

- Altmann, M., Balata, M., Belli, P., et al. 2005, *Physics Letters B*, 616, 174
- Arpesella, C., Back, H. O., Balata, M., et al. 2008, *Physical Review Letters*, 101, 091302
- Asplund, M., Grevesse, N., & Sauval, A. J. 2005, in *Astronomical Society of the Pacific Conference Series*, Vol. 336, *Cosmic Abundances as Records of Stellar Evolution and Nucleosynthesis*, ed. T. G. Barnes, III & F. N. Bash, 25
- Asplund, M., Grevesse, N., Sauval, A. J., & Scott, P. 2009, *ARA&A*, 47, 481
- Badnell, N. R., Bautista, M. A., Butler, K., et al. 2005, *MNRAS*, 360, 458
- Bahcall, J. N., Basu, S., & Serenelli, A. M. 2005, *ApJ*, 631, 1281
- Bahcall, J. N., & Pinsonneault, M. H. 2004, *Physical Review Letters*, 92, 121301
- Bahcall, J. N., Pinsonneault, M. H., & Basu, S. 2001, *ApJ*, 555, 990
- Bahcall, J. N., Serenelli, A. M., & Basu, S. 2006, *ApJS*, 165, 400
- Basu, S., & Antia, H. M. 1997, *MNRAS*, 287, 189
- . 2004, *ApJ*, 606, L85
- . 2008, *Phys. Rep.*, 457, 217
- Basu, S., Chaplin, W. J., Elsworth, Y., New, R., & Serenelli, A. M. 2009, *ApJ*, 699, 1403
- Bellini, G., Benziger, J., Bick, D., et al. 2011, *Physical Review Letters*, 107, 141302
- Bottino, A., Fiorentini, G., Fornengo, N., et al. 2002, *Phys. Rev. D*, 66, 053005
- Caffau, E., Ludwig, H.-G., Steffen, M., Freytag, B., & Bonifacio, P. 2011, *Sol. Phys.*, 268, 255
- Cravens, J. P., Abe, K., Iida, T., et al. 2008, *Phys. Rev. D*, 78, 032002
- Davis, R., Harmer, D. S., & Hoffman, K. C. 1968, *Physical Review Letters*, 20, 1205
- Degl’Innocenti, S., Dziembowski, W. A., Fiorentini, G., & Ricci, B. 1997, *Astroparticle Physics*, 7, 77
- Delahaye, F., & Pinsonneault, M. H. 2006, *ApJ*, 649, 529
- Delahaye, F., Pinsonneault, M. H., Pinsonneault, L., & Zeippen, C. J. 2010, *ArXiv e-prints*, arXiv:1005.0423
- Ferguson, J. W., Alexander, D. R., Allard, F., et al. 2005, *ApJ*, 623, 585
- Fiorentini, G., Ricci, B., & Villante, F. L. 2001, *Physics Letters B*, 503, 121

- Fogli, G. L., Lisi, E., Marrone, A., Montanino, D., & Palazzo, A. 2002, *Phys. Rev. D*, 66, 053010
- Fogli, G. L., Lisi, E., Marrone, A., et al. 2003, *Phys. Rev. D*, 67, 073002
- Fogli, G. L., Lisi, E., Montanino, D., & Palazzo, A. 2001, *Phys. Rev. D*, 64, 093007
- Gonzalez-Garcia, M. C., Maltoni, M., & Salvado, J. 2010, *Journal of High Energy Physics*, 5, 72
- Grevesse, N., & Sauval, A. J. 1998, *Space Sci. Rev.*, 85, 161
- Guzik, J. A., & Mussack, K. 2010, *ApJ*, 713, 1108
- Hampel, W., Handt, J., Heusser, G., et al. 1999, *Physics Letters B*, 447, 127
- Hirata, K. S., Kajita, T., Kifune, K., Kihara, K., & Nakahata, M. 1989, *Physical Review Letters*, 63, 16
- Houdek, G., & Gough, D. O. 2011, *MNRAS*, 418, 1217
- Iglesias, C. A., & Rogers, F. J. 1996, *ApJ*, 464, 943
- Lin, C.-H., Antia, H. M., & Basu, S. 2007, *ApJ*, 668, 603
- Lodders, K. 2010, in *Principles and Perspectives in Cosmochemistry*, ed. A. Goswami & B. E. Reddy, 379
- Ricci, B., & Villante, F. L. 2002, *Physics Letters B*, 549, 20
- Serenelli, A., Peña-Garay, C., & Haxton, W. C. 2013, *Phys. Rev. D*, 87, 043001
- Serenelli, A. M., Basu, S., Ferguson, J. W., & Asplund, M. 2009, *ApJ*, 705, L123
- Serenelli, A. M., Haxton, W. C., & Peña-Garay, C. 2011, *ApJ*, 743, 24
- Thoul, A. A., Bahcall, J. N., & Loeb, A. 1994, *ApJ*, 421, 828
- Turck-Chièze, S., Couvidat, S., Piau, L., et al. 2004, *Physical Review Letters*, 93, 211102
- Villante, F. L. 2010, *ApJ*, 724, 98
- Villante, F. L., Fiorentini, G., & Lisi, E. 1999, *Phys. Rev. D*, 59, 013006
- Villante, F. L., & Ricci, B. 2010, *ApJ*, 714, 944
- Villante, F. L., & Serenelli, A. M. 2013, in preparation
- Vorontsov, S. V., Baturin, V. A., Ayukov, S. V., & Gryaznov, V. K. 2013, *MNRAS*, 430, 1636
- Weiss, A., & Schlattl, H. 2008, *Ap&SS*, 316, 99